

Supporting Information

Targeted intracellular delivery of proteins with spatial and temporal control

Demosthenes P. Morales, Gary B. Braun, Alessia Pallaoro, Renwei Chen, Xiao Huang, Joseph A. Zasadzinski, Norbert O. Reich*

1. Additional Methods and Materials

1.1 HGN Characterization

To measure the size distribution of the hollow gold nanoshells, the particles were visualized by transmission electron microscopy using a FEI Tecnai G2 Sphera microscope operating at 200 kV.

The optical properties were characterized by UV-Vis absorption using a Tecan Infinite 200 Pro microplate reader on a 96-well flat clear bottom plastic plate (BD Biosciences). Using a Nanosight LM10HS (Nanosight, Amesbury, UK) we estimated the HGN to have an extinction coefficient of 3.1×10^{10} at plasmon peak wavelength 800 nm.

1.2 Co-Culture Visualization

PPC-1 and M21 cells were maintained in high glucose Dulbecco's Modified Eagle Medium (DMEM) with phenol red (HyClone) supplemented with 10 % fetal bovine serum (HyClone) at 37°C in 5% CO₂. Prior to co-culture, M21 cells were grown in 12 well plates and stained with 50 μM of CellTracker orange (CTO, Life Technologies) for 30 minutes at 37°C and 5% CO₂, according to the manufacturer's protocol, in serum-free medium. CTO becomes impermeable to the plasma membrane once internalized in the cytosol and is passed to daughter cells at division. M21 cells were then washed 3 times with Dulbecco's phosphate buffered saline (DPBS), collected using a 0.25% trypsin/EDTA solution (Sigma), and plated as stated above. In co-culture experiments the cells were grown together on an 8 well chambered glass slide (Thermo LabTek II) at an initial seeding density of 20,000 PPC-1 and 20,000 M21 (pre-labeled with CTO) cells per well and then incubated for 24 hours at 37°C in 5% CO₂ in complete medium.

Visualization for co-culture utilized both 473 nm blue and 559 nm green laser diodes (15 mW) sequentially to excite GFP and CTO respectively. Cells containing R-GFP-HGN are pseudo-colored green whereas cells containing CTO are pseudo-colored red, unless otherwise stated.

2. Supplemental Figures

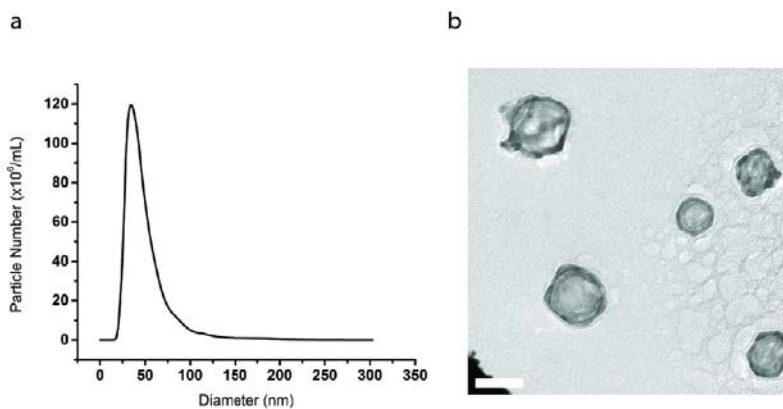


Figure S1: Analysis of HGN

a) HGN were determined to be ~40 nm in diameter by a commercial Nanosight LM10HS. b) Transmission electron microscopy of HGN in inset suggests hollow interior as determined by decreased electron density in the center of the shells.

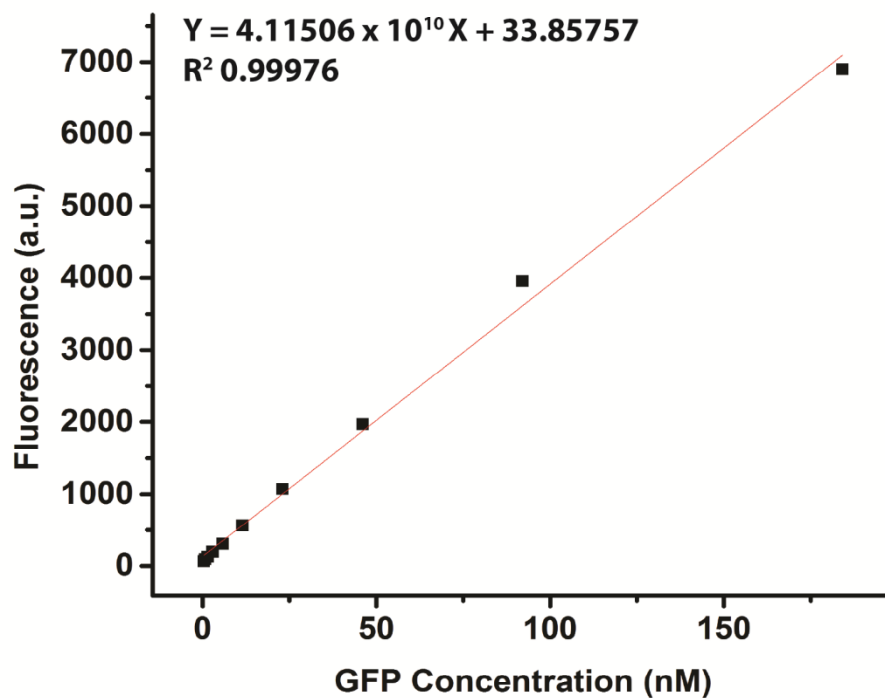


Figure S2: Calibration curve for the quantification of GFP on HGN

The concentration of GFP loaded on HGN and after laser treatment, was evaluated from a standard curve prepared by the serial dilution of a known GFP concentration in 10 mM imidazole buffer.

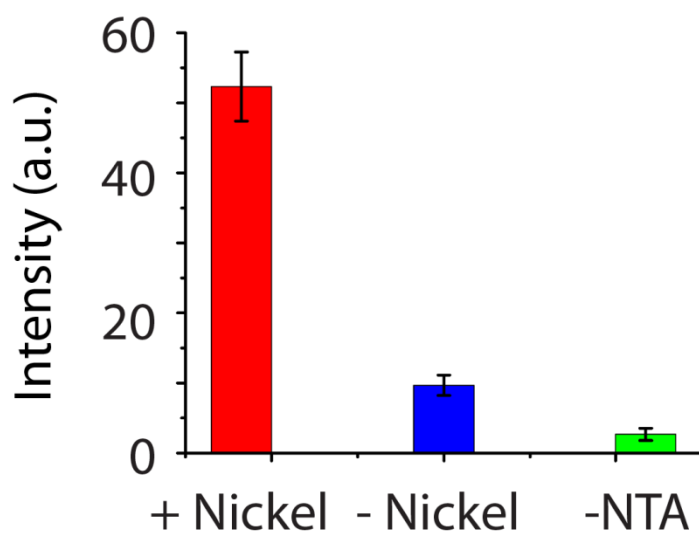


Figure S3: GFP binding to HGN requires nickel

GFP associates with HGN through the formation of coordinate bonds with nickel (Ni^{2+}). GFP-HGN treated with imidazole were incubated for 10 minutes and centrifuged to measure the fluorescence of the supernatant. GFP-HGN with nickel had the highest amount of associated GFP, while HGN without nickel showed minimal binding. Error bars are standard deviation of samples prepared in triplicate.

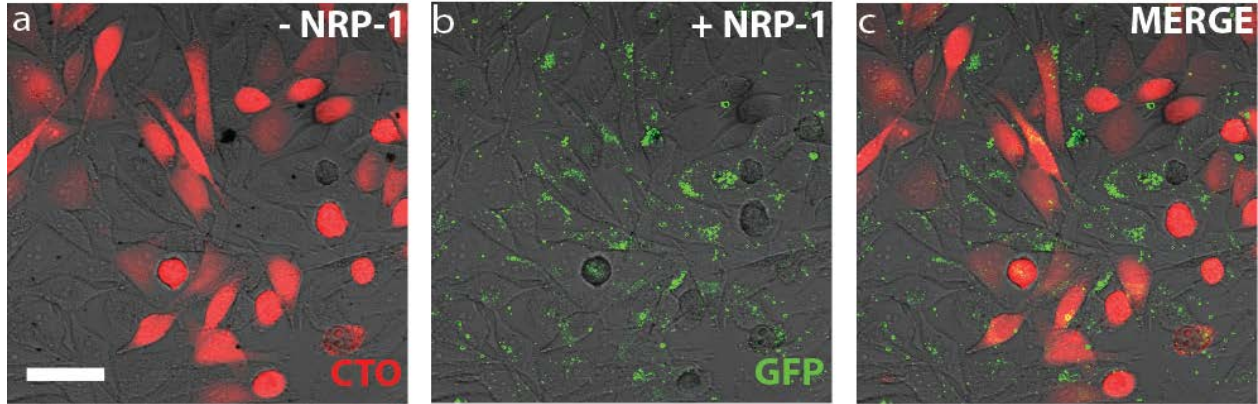


Figure S4. Confocal microscopy imaging of cell-specific targeting of GFP-HGN in a co-culture of NRP-1 receptor-positive PPC-1 and NRP-1 receptor-negative M21 cells. .

PPC-1 and M21 cells were co-cultured on a chambered glass slide to assess the internalization and specificity of the RPARPAR component in the GFP-HGN (GFP-HGN) construct.

Internalization of GFP-HGN into (non-fluorescent) PPC-1 (+NRP-1) was verified by a green punctate fluorescence, suggesting localization within endosomes. Nearly all the PPC-1 cells took up the GFP-HGN, whereas the M21 cells (-NRP-1), labeled with CellTracker orange (CTO) dye showed minimal GFP-HGN association. Scale bar is 50 μm .

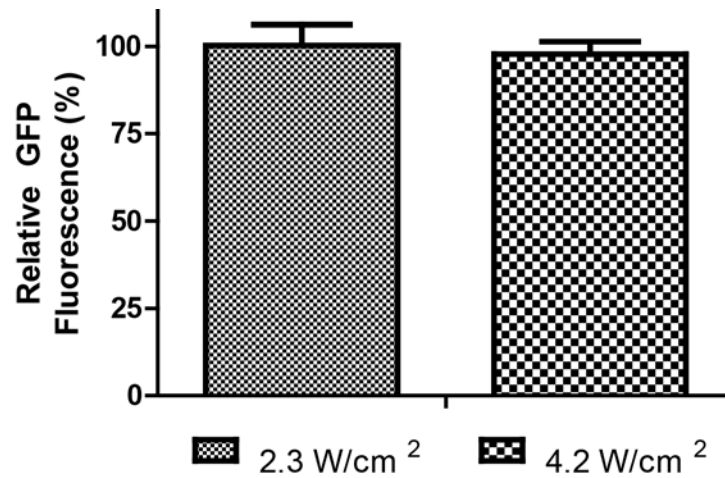


Figure S5: Effect of high laser energy and HGN on GFP fluorescence

Irradiation of free GFP solution exposed to NIR irradiation for 60 seconds with fluence of 2.3 mJ/cm² and 4.2 mJ/cm² at 1000 Hz (fine and coarse hash marks, respectively). Error bars are standard deviation of samples prepared in triplicate.

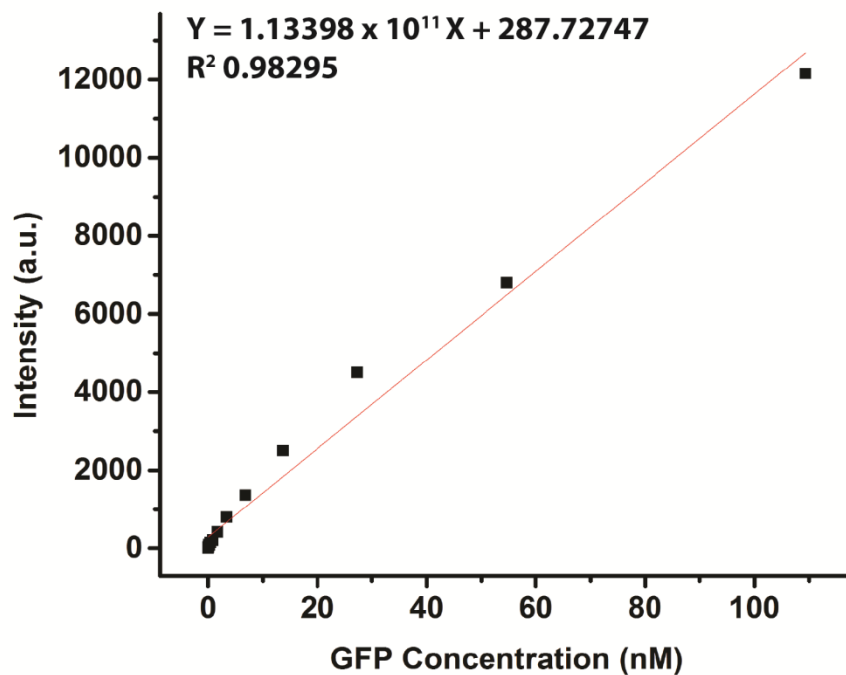


Figure S6: Calibration curve for the quantification of GFP molecules per cell.

The concentration of GFP in cells was quantified using the standard curve generated by the serial dilution of a known GFP concentration in 100 mM imidazole in lysis buffer. The number of GFP molecules was estimated to be $\sim 10^5$ per cell.

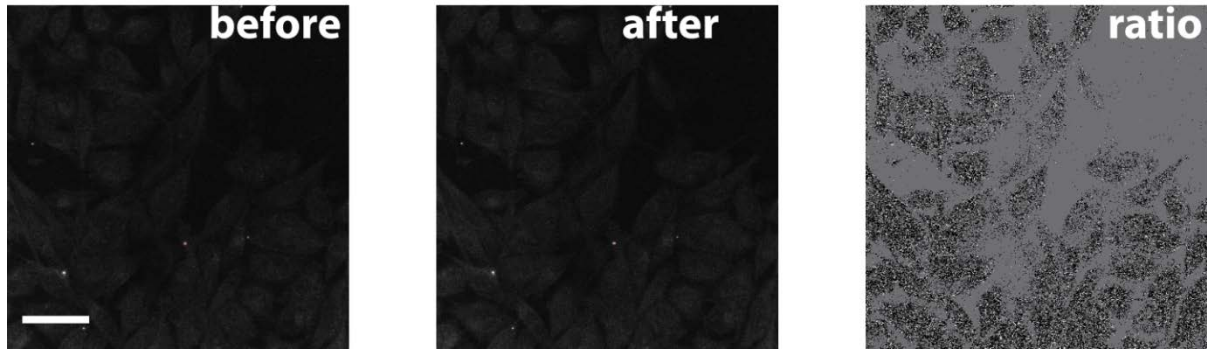


Figure S7: Effect of laser exposure on cell autofluorescence

PPC-1 cells before and after NIR excitation. The black pixels seen in the ratio of the after and before indicates that there is no increased intensity from the autofluorescence of the PPC-1 cells in the green fluorescence channel. Scale bar is 50 μm .

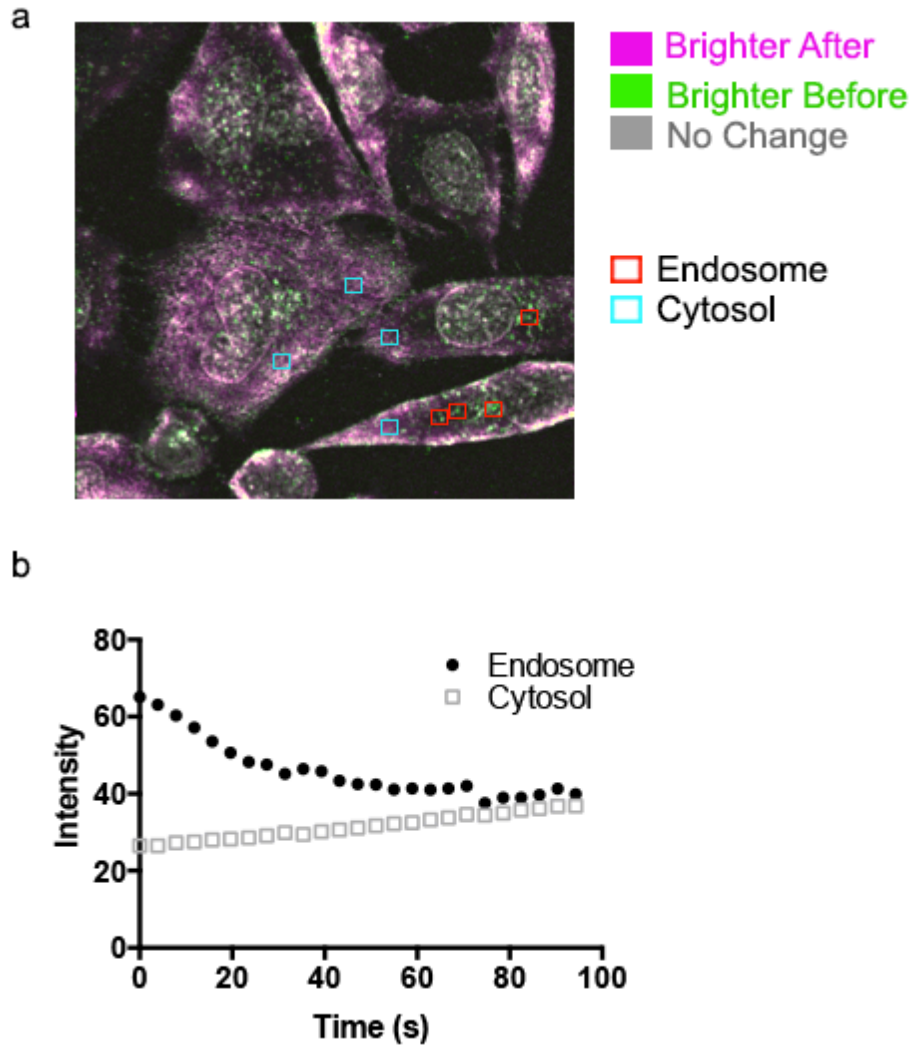


Figure S8. Two-photon real-time imaging of GFP-RP release from GFP-HGN.

Images were captured in the GFP emission channel during two-photon excitation of R-GFP-HGN in PPC-1 cells. Here, the laser causes both the release of R-GFP and captures its fluorescence. (a) Endosome intensity dissipates and cytosolic fluorescence grows. The initial and final frames of a ~100 s movie sequence are shown in green and purple, as an overlay. Pixels which are brighter after laser exposure appear as purple, and those brighter before exposure are green. Unchanged pixels appear gray-white (the combination of green+purple). Endosomes are brighter before the excitation and other regions of the cell are brighter after excitation. (b) Time traces of selected regions in (a) were averaged and plotted. Intensity for each trace was normalized to the initial frame intensity. The results show that endosomes decrease in fluorescence while the cytosol gradually increases, supporting the conclusion that R-GFP was released from endosomes.